Key Engineering Materials
ISSN: 1662-9795, Vol. 944, pp 3-12

Submitted: 2022-10-16
Revised: 2022-12-01
Accepted: 2022-12-06
Online: 2023-04-10

A Comparative Analysis between the Transverse and Longitudinal Samples of the FSW AA5083/AA6082 Joints

Molebogeng Oarabile Mmanyane Segaetsho[1,a*], Velaphi Msomi[1,b] and Vuyani Moni[1,c]

[1]Cape Peninsula University of Technology, Faculty of Engineering and the Built Environment, Mechanical Engineering Department, P. O. Box 1906, 7535, South Africa

[a]segaetshomom@gmail.com, [b]msomiv@gmail.com, [c]vmoni.upc@gmail.com

Keywords: Dissimilar joints; friction stir welding; transverse; longitudinal; macrostructure; microstructure; tensile strength; microhardness.

Abstract. A comparison of middle transverse and longitudinal samples of 6 mm thick FSW AA5083/AA6082 joints is reported in this study. To investigate the differences, the study compares the FSW middle samples obtained from the two orientations to the parent materials through metallographic (macro/microstructure) and mechanical (tensile, micro-hardness) tests. The results revealed that the transverse and longitudinal samples had hardness values of 93.90 and 119.27 HV0.2, respectively, whereas the highest tensile strength of the same samples was 130.694 MPa and 127.833 MPa, with strain values of 0.054 and 0.0834, respectively.

1. Introduction

Friction stir welding (FSW) was first launched to the world in 1991 as a Wayne Thomas invention at TWI (The Welding Institute) [1, 2, 3, 4]. This energy-efficient solid-state approach, which creates joints using a non-consumable welding tool, has witnessed significant growth in various industries since its debut. FSW primarily relies on friction being created between the workpiece and the welding tool, which raises temperatures, causes the materials to plasticize, and makes it easier for the materials to flow while stirring [5]. Once solidified, a joint is created that has physical and chemical capabilities that are equivalent to or improved to those of the parent materials (PM) [6, 7]. One additional and most frequently cited reason for the choice to use the FSW application is that it does not require the material to reach a molten state to form joints, as is the case with traditional methods, which results in unsatisfactory outcomes such as structure failure [8, 9, 10].

The FSW method has been described as being cost-effective and having energy-efficient qualities. It does not require shielding gases, filler metals, or post-weld surface treatments like grinding that may be necessary for achieving a good weld in conventional welding procedures [11]. It is also known to allow both similar and dissimilar joints out of complex and heat-sensitive materials, such as aluminium and its alloys, to be produced without difficulty, as observed when using conventional methods [12]. This feature allows for the production of joints with improved product features and performance and has been documented by several studies.

Nautical, aeronautical, manufacturing and architectural engineering are only a few diverse industries where the FSW application has expanded due to the method's superior material and physical enhancing qualities [13]. The characteristics of the joints and the weld properties have been examined using a variety of techniques and different approaches, including joint examinations in the traversing, diagonal, and longitudinal directions [14]. However, most research has concentrated mainly on the joints' tensile characteristics. Without saying, this has limited the greater part of the understanding of FSW joints to tensile characteristics [15,16]. Various works have been conducted where the FSW technique was used to fabricate dissimilar joints between A5083 and AA6082. This includes the optimization of the process parameters and also looking at the correlation between a single parameter to the mechanical response of the developed joint. Donatus et al. [17] have analyzed the variations in the thermomechanically affected zone of the dissimilar friction stir welded AA5083 and 6082 joints. The major focus of this analysis was based on the major alloying elements of each material, and the samples analyzed were sampled in one direction. It was discovered that the Mg content is slightly affected for both materials. This has compromised some of the mechanical properties like tensile strength and microhardness.

Kumar and Ramana [18] have investigated the influence of tool parameters on the tensile strength of AA5083/AA6082 dissimilar joints. The tensile analysis was conducted on the sampled samples perpendicular to the welding direction. It was discovered that the tensile properties were more highly dependent on the shoulder diameter than any other parameters. This discovery resulted in the development of a mathematical equation that can relate the tensile properties to the tool's parameters. Leitao et al. [19] have investigated the weldability of AA5083 and AA6082 under different conditions with a major focus on high-temperature plastic behaviour. The mechanical properties were examined on the samples that were sampled perpendicular to the welding direction. It was discovered that the difference in mechanical properties of each material was getting closer to each other with the increase in temperature. The mechanical behaviour of similar and dissimilar AA5083 and AA6082 joints was analyzed by Gungor et al. [20]. The mechanical analysis was conducted on the sampled samples perpendicular to the welding direction. The similar joints were studied comparatively to the dissimilar joints. It was discovered that the alternating mechanical behaviour was greatly influenced by the combination of rotational speed and welding speed. It should be noted that there is a limited work where FSW was used to fabricate dissimilar joints between AA5083 and AA6082 but the majority of works report on one of the mentioned materials mixed with other metals.

In as much as there are works that dealt with different analysis of joint formed between AA5083 and AA6082 through FSW technique, there is no work that has analyzed the mechanical properties of the same joint with the focus of sampling direction. This is critical to understand the weakness and the strength of the joint in terms of loading direction. This study compares the tensile, micro-hardness, and macro/microstructure of middle longitudinal (LM) and middle transverse (TM) samples from the AA5083-H321 / AA6082-T651 joint. This is due to their widespread use in the industry due to their exceptional mechanical and metallurgical qualities, aluminium, and its alloys are among the most studied materials [10, 21, 22].

2. Materials, Welding Preparations and Parameters

The chemical compositions of the aluminium alloys AA5083-H321 and AA6082-T651 were determined using a Belec Compact Port Hybrid Low Carbon (HLC) Spectrometer, whose results are shown in Table 1. A Lagun FA. 1-LA conventional vertical milling machine was used to fabricate a joint using 6 mm thick blanks of materials AA5083 (460 x 70 mm) and AA6082 (510 x 70 mm) at rotational and transverse speeds of 900 rpm and 60 mm/min, respectively. On the fixture, the blanks were positioned with AA5083 on the advancing and AA6082 on the retreating side as depicted in Fig.1(a). At a tool tilt angle of 1°, a square threaded high-speed steel tool with 6 mm tool pin diameter, 5.8 mm tool pin length, and 20 mm tool shoulder diameter was applied. The FSW joint was fabricated, as indicated in Fig. 1(b). A water jet was used to extract all samples, including those that are being described in this research, such as metallographic and hardness samples, from the beginning, middle, and end of the work piece in two directions: perpendicular and longitudinal to the welded connection. Sample designs were created using SOLIDWORKS 2018 3D software.

Table 1: AAA5083 and AA6082 chemical compositions.

	Al	Si	Fe	Cu	Mn	Mg	Cr	Zn	Ti
5083	Balance	0.148	0.163	0.015	0.684	4.022	0.040	0.011	0.017
6082	Balance	1.329	0.679	0.026	0.433	1.209	0.005	0.544	0.042

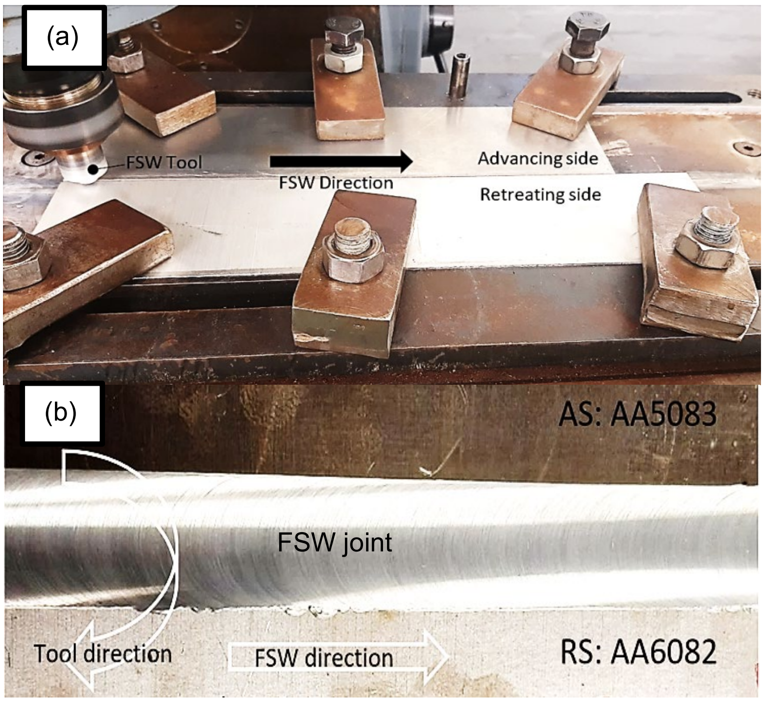

Figure 1: (a) FSW setup and (b) FSW joint.

3. Sampling and Sample Preparations

The American Society for Testing and Materials (ASTM) standards were used for sample design and testing guidelines. ASTM E8M-04 was employed for testing tensile samples, ASTM E384-11 was used to test hardness samples, and ASTM E112-12 was employed in evaluating the median grain size. The macrostructure images were taken using a Zeiss Stemi 2000CS Stereo microscope Binocular, and the microstructure of the welded joints was examined with a Motic AE 200 microscope and Motic software at magnifications of 5 and 100 on a scale of 100 µm. The metallographic and micro-hardness samples were extracted separately to prevent having to repeat the metallographic method on the samples, with the micro-hardness preparation leading only up to 3 µm. The metallographic method for the macro/microstructural samples included grinding and polishing prior to etching, using a variety of grinding and polishing discs (from P230 to Aka-Chemal) and media (distilled water to Aka-Lube) on the Struers LaboPol-5. Two etching solutions were employed to elucidate the structure of the samples: pre-etch sodium hydroxide (2g Sodium hydroxide (NaOH) and 100 ml distilled water (H2O)) and Weck's reagent (1g Sodium hydroxide (NaOH), Potassium Permanganate (KMnO4) and 100 ml distilled water (H2O)). On the transverse samples, the parent AA6082 and a section of the weld zone on its side were exposed to sodium hydroxide for six seconds, while the parent AA5083 was covered with masking tape. After removing the tape, Weck's agent was used to etch the whole sample for six minutes. The same agents were employed for longitudinal sampling, however due to the material's fast reactivity from the relatively small quantities that were in layers, a different approach had to be used. This technique included employing sodium hydroxide for two seconds to evade over-etching during the Weck’s application which was done for five minutes. The hardness tests were performed using the InnovaTest Falcon 500 hardness testing equipment with a 0.2-kilogram force and nineteen indentations in each of three lines at a dwell time of ten seconds.

4. Materials, Welding Preparations And Parameters

4.1. Macro/ microstructure analysis

Fig. 2(a) and (b) show the middle transverse (TM) and middle longitudinal (LM) macrostructure sections obtained from the joint, respectively. Figure 2(a) depicts the various zones of FSW as previously discovered by FSW researchers who investigated a variety of materials [23-25]. In this context, however, the image simply depicts two of the key zones, the Stir Zone (SZ) and Thermo-Mechanically Affected Zone (TMAZ) which is more apparent on the advancing side than the retreating side, with no apparent SZ housing onion rings. A route of inter-material flow represented by streaks of materials in the SZ was also noticed. Figure 2(b) depicts the longitudinal sample where materials are arranged in layers. The traversing and rotational motion of the tool and tool pin rip and propel the soft material in layers from the parent materials, which subsequently flow between the threads of the tool [26]. Further examination of the sample revealed the presence of a tunnel defect at the bottom of the joint shrunk towards the retreating side of the sample. Several researchers have indicated that this defect is a result of incompatible parameters causing poor material flow, exacerbated by derisory heat input [27, 28]. This suggests that the pressure and temperature were insufficient to prevent the occurrence of the tunnel defect, which can be seen running the length of the sample sectioned longitudinally in Figure 2(b) [29]. The samples also included micro-cavities that are encircled in Fig. 2(a) and 2(b). These may were identified at the materials' interface in the longitudinal sample and on the advancing side of the traverse sample.

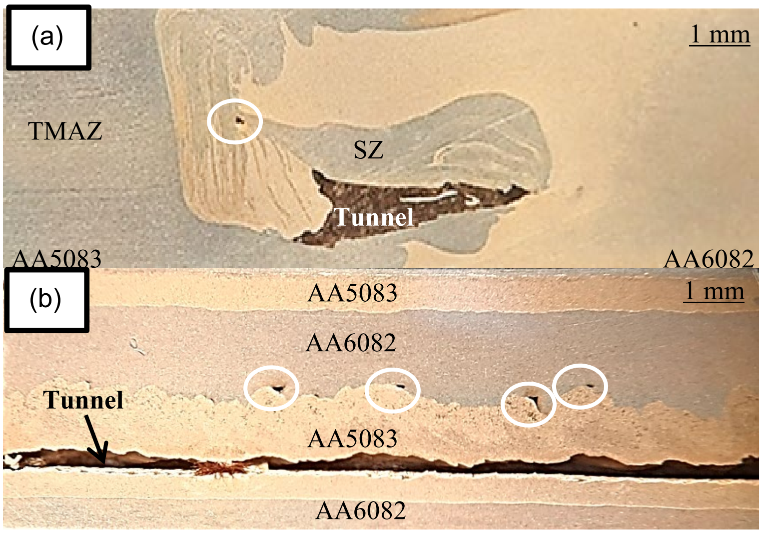

Figure 2: Macrographs, (a) FS welded transverse and (b) FS welded longitudinal samples.

The configuration for obtaining pictures from the samples is shown in Fig. 3(a) and 3(b), and the position from where they were obtained is denoted by BL2.

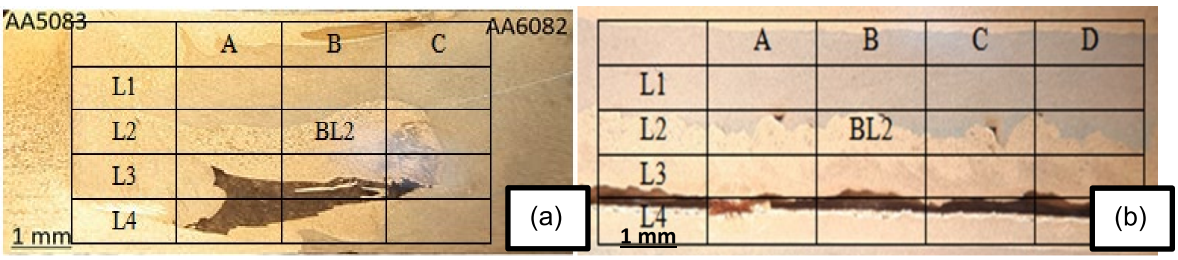

Figure 3: Macrographs, (a) FS welded transverse and (b) FS welded longitudinal samples.

Fig. 4 (a) and 4 (b) depict the micro-images of the traverse samples. Figure 4(a) shows the traverse sample where it can be clearly seen that the SZ and TMAZ are clearly separated by a boundary line. This can be the result of particles building up due to uniformly dispersion during application [30]. The TMAZ materials appear as a zone of contouring grains that are aligned rotated in the opposite direction (almost diagonal) to the SZ material. Unmixed but more refined materials of AA5083 and AA6082 than those found from the parent materials (PM) are shown in Fig. 4(b). It is quite clear that there was no mixing of the materials, only inter-material movement as depicted in Figure 4 (b) [2, 31, 32]. The longitudinal samples are displayed in Fig. 4(c) and 4(d). Given that the original grains of AA5083 characterized by column grains and those of AA6082 characterized by flat, oblong grains, it is clear from the micro-images that the materials have undergone grain refining. This alteration or refinement is due to the significant frictional material calefaction and distortion during the welding process, which aids dynamic recrystallization of grains, and introduces the contrast in the stir zone [33]. The refinement of grains in joints has reportedly been associated to an enhancement of their strength or hardness [34]. Similar results are shown in Fig. 4(d), which, like Fig. 4(b), shows that there was no material mixing, but rather inter-flow of materials, as seen by the difference in material textures between AA5083 and AA6082, where AA5083 seems to have somewhat lumpy-looking grains. PMs AA5083 and AA6082 obtained mean grain diameters of 97.385 and 130.832 µm, respectively with a standard deviation of 29.522 and 50.066 µm respectively. The longitudinal sample, exclusively being the sectioned SZ had a mean grain dimension of 41.130 µm and a standard deviation of 22.067 µm, whereas that of transverse SZ had a mean grain dimension of 45.485 µm and a standard deviation of 19.238 µm.

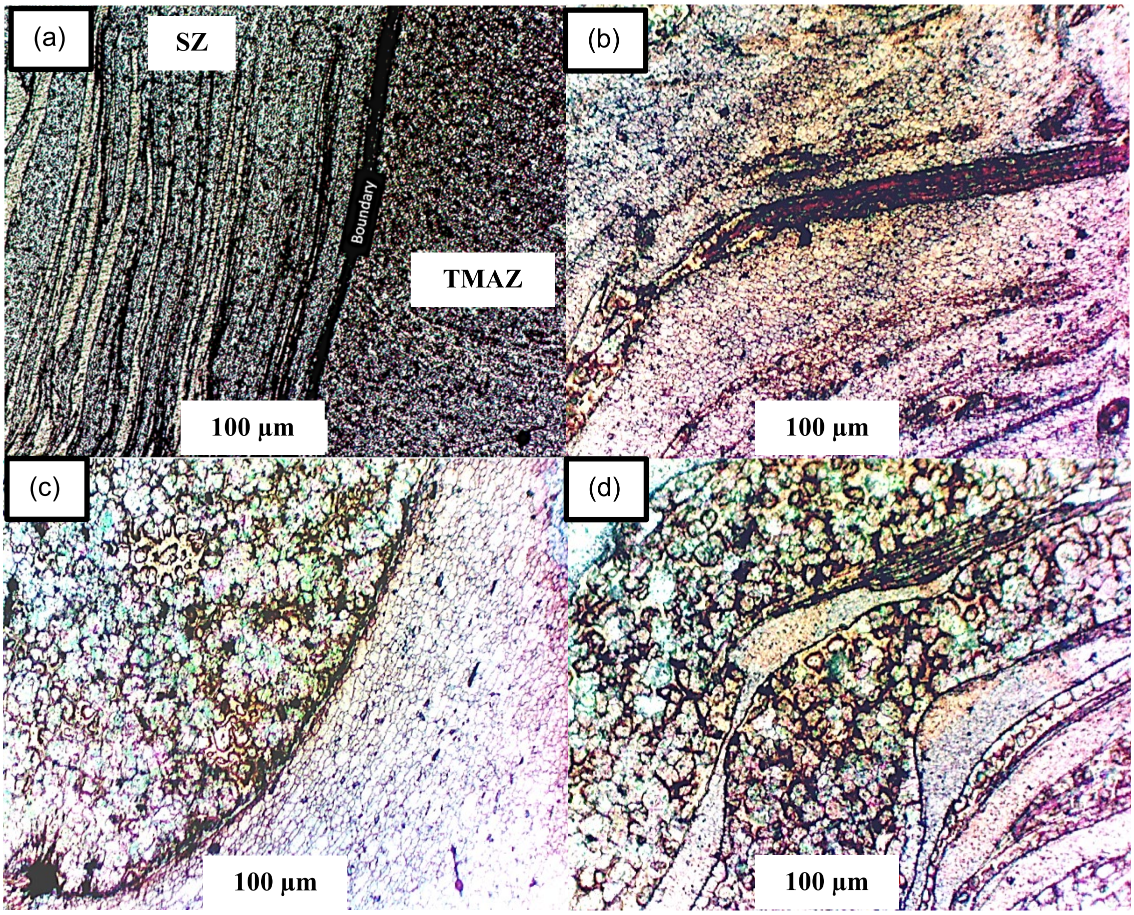

Figure 4: Macrographs, (a) FS welded transverse and (b) FS welded longitudinal samples.

4.2. Microhardness analysis

In this subsection, the samples from the aforementioned joint's micro-hardness characteristics are looked at. As opposed to the parents' samples, with two rows of seventeen indentations, three rows of nineteen indentations impression were made on the joint samples. Average values were employed for the PM results, and the investigations on the joint samples were based on the second row indentations. Fig. 5 displays the profiles of the PMs, transverse samples, and longitudinal samples. Each of the PMs had an average hardness of 155.82 $HV_{0.2}$ for AA5083 and 162.99 $HV_{0.2.}$ for AA6082. Additionally, the hardness of LM and TM samples was evaluated; the mean value for

LM samples was 119.27 $HV_{0.2}$ and 93.90 $HV_{0.2}$, respectively. The hardness of the joint samples was shown to decrease when compared to the outcomes of the tested PMs, as depicted in the graph. This resulted from the distribution and accessibility of precipitates, which affect material characteristics such as alloy strength and hardness when subjected to heat treatment [2]. The decrease in sample hardness at the TMAZ may have been caused by uneven heat distributions, which are known to alter and proliferate the grains in the region especially in heat treated materials. This effect was seen on the longitudinal sample results assuming that the position of the objectives was on AA6082 material when the results were taken.

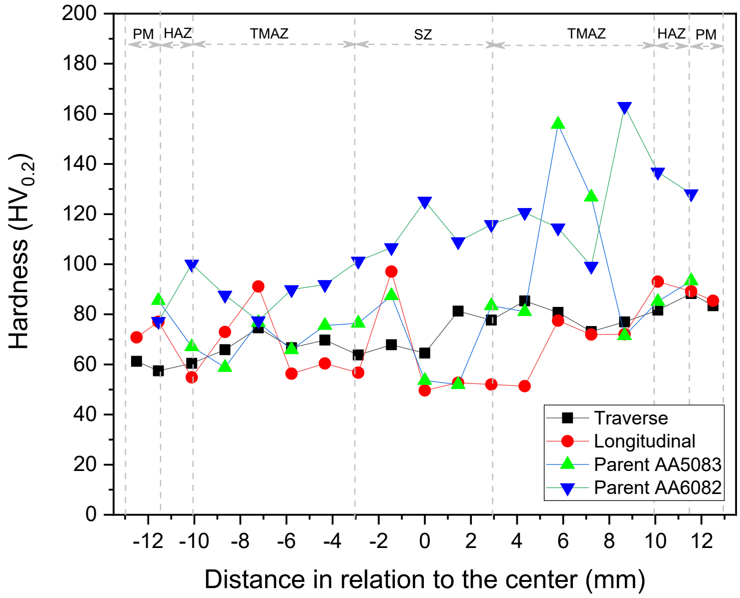

Figure 5: Hardness profiles.

4.3. Mechanical Analysis

Fig. 6 depicts the post-tested tensile test TM and LM samples. At the gripping end of the gauge, the LM sample was shown to exhibit cup-and-cone fracture effect, which indicates that a ductile fracture took place [35, 36]. The TM sample also failed, particularly on the SZ, as expected given the tunnel flaw in the samples. The tensile considering the SZ is elucidated by coinciding findings of the hardness test, which indicate decreased hardness near the joint's centre [37]. Although it is widely understood that the weakest point in the joint would be on the HAZ of the softer material, micro defects, in addition to coarser grains at the bottom at the lower end of the SZ, could have caused the joint to fail [38, 39]. Despite the differences in sampling direction, both the TM and LM samples had a meandering fracture. The stress-strain results of the TM and LM samples are shown in Fig. 7. At strain values of 0.054 and 0.0834, the TM and LM samples achieved maximum tensile strengths of 130.694 MPa and 127.833 MPa, respectively.

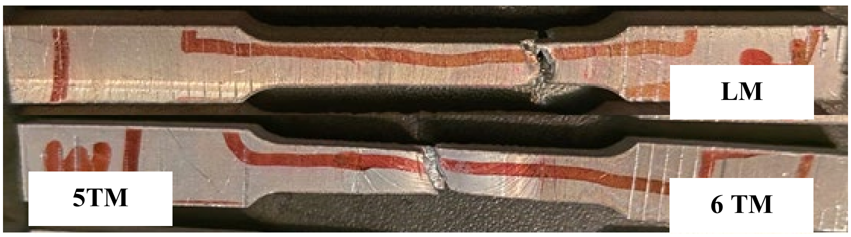

Figure 6: Tested tensile samples.

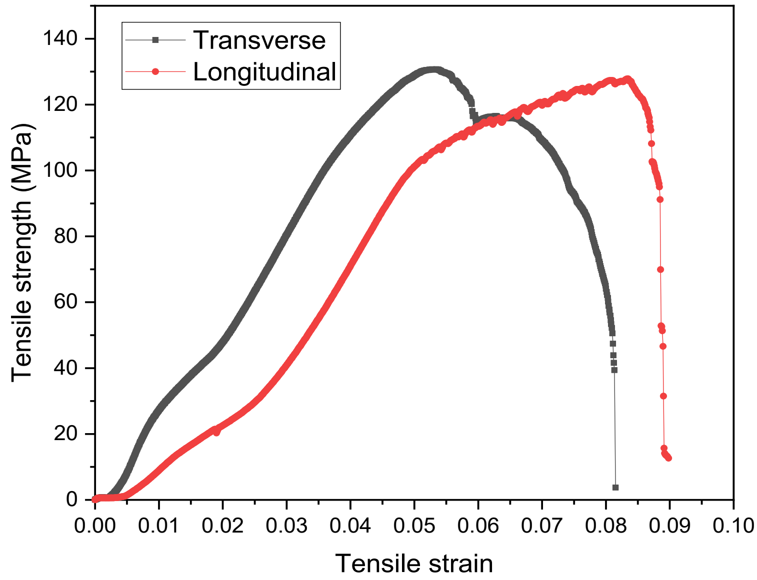

Figure 7: Stress-strain curves.

Conclusion

A reasonable comparison of the TM and LM samples of the FSW AA5083/AA6082 joints was conducted. The following conclusion can be drawn from the results:

- Both the TM and LM samples were observed to have a tunnel and micro-void defects. Despite these defects, the LM and TM samples had comparable joint outcomes. The areas (SZ and TMAZ) of FSW joints were identified from the macro/microstructural analysis.
- Microstructural analysis revealed refined grains compared to the parent materials, and the refined grains are due to dynamic recrystallization.
- The microhardness for both sample directions was lower compared to that of the PMs, and this may be attributed to the strengthening mechanism that was affected by the temperature during the procedure.
- The transverse sample from the tensile sample was shown to fracture at its center (SZ), showing that the region of the weld nugget was weaker than the other regions. This was determined to possibly be the result of defects (tunnel and micro-voids) identified during the macro/microstructural examination. It was noted that the LM sample failed along the gauge, not far from the gripping end of the tensile sample. This can further be investigated to understand the possible cause for the sample to fracture in that particular position.

Future Work

Future work can include the variation of parameters and the positioning to better understand the most influential parameter to the joint quality. The XRD can also be included to verify the phases that may have been formed during the procedure. The temperature profile may also be included during the analysis to strengthen the argument of precipitates.

Acknowledgment

The authors would like to thank the Cape Peninsula University of Technology, Mechanical Engineering Department workshop for their technical assistance.

References

[1] Kallee, S.W., Lohwasser, D. and Chen, Z., 2010. *Friction Stir Welding-from basics to application.*

[2] Sundaram, N.S. and Murugan, N., 2010. *Tensile behavior of dissimilar friction stir welded joints of aluminium alloys*. *Materials & Design*, *31*(9), pp.4184-4193.

[3] Abnar, B., Kazeminezhad, M. and Kokabi, A.H., 2015. *Effects of heat input in friction stir welding on microstructure and mechanical properties of AA3003-H18 plates.* Transactions of Nonferrous Metals Society of China, 25(7), pp.2147-2155.

[4] Al-Roubaiy, A.O., Nabat, S.M. and Batako, A.D., 2020. *An Investigation into Friction Stir Welding of Aluminium Alloy 5083-H116 Similar Joints*. Materials Today: Proceedings, 22, pp.2140-2152.

[5] Ghiasvand, A., Noori, S.M., Suksatan, W., Tomków, J., Memon, S. and Derazkola, H.A., 2022. *Effect of Tool Positioning Factors on the Strength of Dissimilar Friction Stir Welded Joints of AA7075-T6 and AA6061-T6.* Materials, 15(7), p.2463.

[6] Feng, A.H., Xiao, B.L. and Ma, Z.Y., 2008. *Effect of microstructural evolution on mechanical properties of friction stir welded AA2009/SiCp composite.* Composites Science and Technology, 68(9), pp.2141-2148.

[7] Jannet, S., Mathews, P.K. and Raja, R., 2013. *Comparative investigation of friction stir welding and fusion welding of 6061-T6 and 5083-O aluminum alloy based on mechanical properties and microstructure.* Journal of achievements in materials and manufacturing engineering, 61(2), pp.181-186.

[8] Buffa, G., Fratini, L. and Ruisi, V., 2009. *Friction stir welding of tailored joints for industrial applications*. International Journal of Material Forming, 2(1), pp.311-314.

[9] Ullegaddi, K., Murthy, V. and Harsha, R.N., 2017. *Friction stir welding tool design and their effect on welding of AA-6082 T6.* Materials Today: Proceedings, 4(8), pp.7962-7970.

[10] Vimalraj, C. and Kah, P., 2021. *Experimental review on friction stir welding of aluminium alloys with nanoparticles. Metals*, 11(3), p.390.

[11] Albannai, A., 2020. *Review the common defects in friction stir welding.* Int. J. Sci. Technol. Res, 9, pp.318-329.

[12] Shojaeefard, M.H., Behnagh, R.A., Akbari, M., Givi, M.K.B. and Farhani, F., 2013. *Modelling and Pareto optimization of mechanical properties of friction stir welded AA7075/AA5083 butt joints using neural network and particle swarm algorithm.* Materials & Design, 44, pp.190-198.

[13] Saeidi, M., Barmouz, M. and Givi, M.K.B., 2015. *Investigation on AA5083/AA7075+ Al 2 O 3 joint fabricated by friction stir welding: characterizing microstructure, corrosion and toughness behavior*. Materials Research, 18, pp.1156-1162.

[14] Imam, M., Biswas, K. and Racherla, V., 2013. *Effect of weld morphology on mechanical response and failure of friction stir welds in a naturally aged aluminium alloy*. Materials & Design, 44, pp.23-34.

[15] Garg, A., Raturi, M. and Bhattacharya, A., 2019. *Experimental and finite element analysis of progressive failure in friction stir welded AA6061-AA7075 joints.* Procedia Structural Integrity, 17, pp.456-463.

[16] Ramanjaneyulu, K., Madhusudhan Reddy, G., Venugopal Rao, A. and Markandeya, R., 2013. *Structure-property correlation of AA2014 friction stir welds: role of tool pin profile.* Journal of materials engineering and performance, 22(8), pp.2224-2240.

[17] Donatus, U, Thompson, G.E., Momoh, M.I., Maledi, N.B., Tsai, I-L., Ferreira, R.O., Liu, Z., 2018. *Variations in stir zone and thermomechanically affected zone of dissimilar friction stir weld of AA5083 and AA6082 alloys*, Transactions of Nonferrous Metals Society of China 28(12), pp.2410-2418.

[18] Kumar, H.M.A., Ramana, V.V., 2020. *Influence of tool parameters on the tensile properties of friction stir welded aluminium 5083 and 6082 alloys*, Materials Today: Proceedings 27(2), pp.951-957.

[19] Leitão, C., Louro, R., Rodrigues, D.M, 2012. *Analysis of high temperature plastic behaviour and its relation with weldability in friction stir welding for aluminium alloys AA5083-H111 and AA6082-T6*, Materials & Design, 37, pp.402-409.

[20] Gungor, B., Kaluc, E., Taban,E., Sik,A., 2014. *Mechanical, fatigue and microstructural properties of friction stir welded 5083-H111 and 6082-T651 aluminum alloys*, Materials & Design 56, pp.84-90.

[21] Kim, S., Lee, C.G. and Kim, S.J., 2008. *Fatigue crack propagation behavior of friction stir welded 5083-H32 and 6061-T651 aluminum alloys*. Materials Science and Engineering: A, 478(1-2), pp.56-64.

[22] Prabha, K.A., Putha, P.K. and Prasad, B.S., 2018. *Effect of tool rotational speed on mechanical properties of aluminium alloy 5083 weldments in friction stir welding*. Materials Today: Proceedings, 5(9), pp.18535-18543.

[23] Kallee, S.W., Lohwasser, D. and Chen, Z., 2010. *Friction Stir Welding-from basics to application.*

[24] Sundaram, N.S. and Murugan, N., 2010. *Tensile behavior of dissimilar friction stir welded joints of aluminium alloys*. *Materials & Design*, *31*(9), pp.4184-4193.

[25] Abnar, B., Kazeminezhad, M. and Kokabi, A.H., 2015. *Effects of heat input in friction stir welding on microstructure and mechanical properties of AA3003-H18 plates.* Transactions of Nonferrous Metals Society of China, 25(7), pp.2147-2155.

[26] Al-Roubaiy, A.O., Nabat, S.M. and Batako, A.D., 2020. *An Investigation into Friction Stir Welding of Aluminium Alloy 5083-H116 Similar Joints*. Materials Today: Proceedings, 22, pp.2140-2152.

[27] Rajaseelan, S.L. and Kumarasamy, S., 2020. *Mechanical Properties and Microstructural Characterization of Dissimilar Friction Stir Welded AA5083 and AA6061 Aluminium Alloys.* Mechanics, 26(6), pp.545-552.

[28] Kalemba-Rec, I., Hamilton, C., Kopyściański, M., Miara, D. and Krasnowski, K., 2017. *Microstructure and mechanical properties of friction stir welded 5083 and 7075 aluminum alloys*. Journal of Materials Engineering and Performance, 26(3), pp.1032-1043.

[29] Elatharasan, G., Manikandan, R. and Karthikeyan, G., 2021. *Multi-response optimization of process parameters in friction stir welding of dissimilar aluminum alloys by Grey relation analysis (AA 6061-T6 & AA5083-H111).* Materials Today: Proceedings, 37, pp.1172 1182.

[30] Saeidi, M., Barmouz, M. and Givi, M.K.B., 2015. *Investigation on AA5083/AA7075+ Al 2 O 3 joint fabricated by friction stir welding: characterizing microstructure, corrosion and toughness behavior*. Materials Research, 18, pp.1156-1162.

[31] Albannai, A., 2020. *Review the common defects in friction stir welding.* Int. J. Sci. Technol. Res, 9, pp.318-329.

[32] Feng, A.H., Xiao, B.L. and Ma, Z.Y., 2008. *Effect of microstructural evolution on mechanical properties of friction stir welded AA2009/SiCp composite.* Composites Science and Technology, 68(9), pp.2141-2148.

[33] Jannet, S., Mathews, P.K. and Raja, R., 2013. *Comparative investigation of friction stir welding and fusion welding of 6061-T6 and 5083-O aluminum alloy based on mechanical properties and microstructure.* Journal of achievements in materials and manufacturing engineering, 61(2), pp.181-186.

[34] Shojaeefard, M.H., Behnagh, R.A., Akbari, M., Givi, M.K.B. and Farhani, F., 2013. *Modelling and Pareto optimization of mechanical properties of friction stir welded AA7075/AA5083 butt joints using neural network and particle swarm algorithm.* Materials & Design, 44, pp.190-198.

[35] Sithole, K. and Rao, V.V., 2016. *Recent developments in micro friction stir welding: a review.* In IOP conference series: materials science and engineering (Vol. 114, No. 1, p.012036). IOP Publishing.

[36] Buffa, G., Fratini, L. and Ruisi, V., 2009. *Friction stir welding of tailored joints for industrial applications*. International Journal of Material Forming, 2(1), pp.311-314.

[37] Ullegaddi, K., Murthy, V. and Harsha, R.N., 2017. *Friction stir welding tool design and their effect on welding of AA-6082 T6.* Materials Today: Proceedings, 4(8), pp.7962-7970.

[38] Vimalraj, C. and Kah, P., 2021. *Experimental review on friction stir welding of aluminium alloys with nanoparticles. Metals*, 11(3), p.390.

[39] Kim, S., Lee, C.G. and Kim, S.J., 2008. *Fatigue crack propagation behavior of friction stir welded 5083-H32 and 6061-T651 aluminum alloys*. Materials Science and Engineering: A, 478(1-2), pp.56-64.